



Preparation and characterization of cobalt-containing *P,N*-ligands and an unusual palladium complex ion pair: their applications in amination reactions

You-Chen Hsiao, Wen-Yuan Chiang, Chia-Ming Weng, Fung-E Hong*

Department of Chemistry, National Chung Hsing University, Taichung 40227, Taiwan

ARTICLE INFO

Article history:

Received 11 April 2008

Received in revised form 17 July 2008

Accepted 18 July 2008

Available online 23 July 2008

Keywords:

Bidentate ligand
Palladium complex
Cobalt complex
dppm

ABSTRACT

Several cobalt-containing *P,N*-ligands, alkyne-bridged dicobalt phosphines [(μ-PPh₂CH₂PPh₂)Co₂(CO)₄(μ,η-Me₂NCH₂C≡CPR₂)] (**4a**: R=^tBu; **4b**: R=Ph; **4c**: R=Cy), were prepared from the reactions of corresponding alkynylphosphines Me₂NCH₂C≡CPR₂ (**2a**: R=^tBu; **2b**: R=Ph; **2c**: R=Cy) with a dppm-bridged dicobalt complex [Co₂(CO)₆(μ-P,P-PPh₂CH₂PPh₂)] **3**. A unique palladium complex ion pair [(μ-PPh₂CH₂PPh₂)Co₂(CO)₄(μ,η-Me₂NCH₂C≡CP(^tBu)₂)Pd(η³-C₃H₅)]⁺[(η³-C₃H₅)PdCl₂]⁻ **7a** was obtained from the reaction of **4a** with [(η³-C₃H₅)PdCl₂]₂. Compounds **4a**, **4b**, and **4c** are authentic cobalt-containing *P,N*-bidentate ligands and can be used for ligation of palladium from various sources such as Pd(OAc)₂ or [(η³-C₃H₅)PdCl₂]₂. Satisfactory efficiencies were observed for the amination reactions of aryl bromides with morpholine employing either a **4a**-chelated palladium complex formed in situ or pre-formed **7a** as the catalytic precursor.

© 2008 Elsevier Ltd. All rights reserved.

1. Introduction

For decades, mono- or multidentate phosphines have been the most frequently employed ligands in the catalytic reactions mediated by ligand-assisted transition metals.¹ Bidentate phosphines have been found to be crucial to the development of their asymmetric versions.^{10–x} However, most of the trialkyl- or triarylphosphines are subjected to oxidation resulting in phosphine oxides whose coordinating capacities toward low-valence transition metals are greatly diminished. Lately, the subject of employing *P,N*-bidentate ligands, which contain both P- and N-coordination sites, in the chelation of transition metals has attracted a great deal of attention.² The advantages of a phosphine possessing both P- and N-coordination sites are obvious. For one thing, these *P,N*-bidentate ligands are less air-sensitive than 'pure' phosphines. More importantly, the relatively ease of formation and dissociation of the *P,N*-metal complex is a useful feature in various catalytic reactions.³ Our previous work has demonstrated that a *P,N*-compound, diphenyl-2-pyridylphosphine, could be employed as a bidentate ligand in the coordination of dicobalt or tetracobalt octacarbonyl complexes.⁴

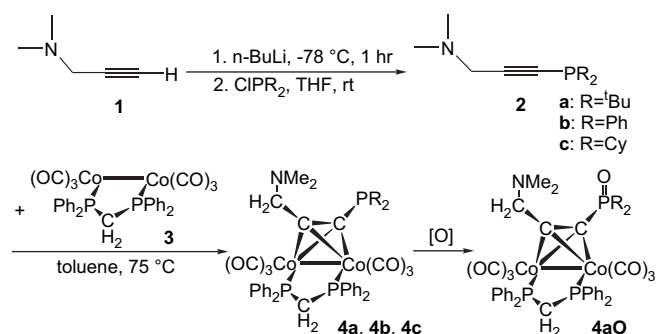
In this work, the preparation of several cobalt-containing bidentate ligands bearing *P,N*-coordination sites is presented. Their capabilities as effective chelating ligands in the palladium-catalyzed amination reactions are demonstrated. Most interestingly,

the characterization of a unique palladium complex ion pair and its use as a catalyst in the amination reaction are also reported.

2. Results and discussion

2.1. Preparation of cobalt-containing *P,N*-ligands **4a**, **4b**, and **4c**

Several alkynylphosphines Me₂NCH₂C≡CPR₂ (**2a**: R=^tBu; **2b**: R=Ph; **2c**: R=Cy) were synthesized from Me₂NCH₂C≡CH **1** according to the published methods with minor modifications (Scheme 1).⁵ Further treatment of a dppm-bridged dicobalt compound [Co₂(CO)₆(μ-P,P-PPh₂CH₂PPh₂)] **3** with 1 mol equiv of **2a** (or **2b**, **2c**) in toluene at 75 °C afforded an alkyne-bridged dicobalt



Scheme 1.

* Corresponding author. Fax: +886 4 22862547.

E-mail address: fehong@dragon.nchu.edu.tw (F.-E. Hong).

Table 1
Crystal data of **4aO**, **4b**, **4c**, and **7a**

Compound	4aO	4b	4c	7a
Formula	C ₄₂ H ₄₈ Co ₂ NO ₅ P ₃	C ₄₆ H ₄₅ Co ₂ NO ₄ P ₃	C ₄₆ H ₅₂ Co ₂ NO ₄ P ₃	C ₄₈ H ₅₆ Cl ₂ Co ₂ NO ₄ P ₃ Pd ₂
Formula weight	857.58	881.5	893.66	1205.45
Crystal system	Monoclinic	Monoclinic	Monoclinic	Triclinic
Space group	<i>P</i> 2(1)/ <i>c</i>	<i>P</i> 2(1)/ <i>n</i>	<i>P</i> 2 ₁ / <i>c</i>	<i>P</i> -1
<i>a</i> (Å)	18.3005(14)	12.1342(11)	13.4495(13)	13.5091(7)
<i>b</i> (Å)	20.7459(17)	23.870(2)	33.378(3)	14.3027(8)
<i>c</i> (Å)	22.8123(19)	15.3841(14)	10.9190(11)	15.1227(9)
α (°)	—	—	—	74.6980(10)
β (°)	93.299(2)	103.516(2)	113.466(2)	64.1460(10)
γ (°)	—	—	—	76.6160(10)
<i>V</i> (Å ³)	8646.6(12)	4332.5(7)	4496.4(8)	2513.4(2)
<i>Z</i>	4	4	4	2
<i>D_c</i> (Mg/m ³)	1.293	1.269	1.320	1.598
λ (MoK α) (Å)	0.71073	0.71073	0.71073	0.71073
μ (mm ⁻¹)	0.917	0.549	0.886	1.597
θ range (°)	1.70–26.04	1.71–26.02	1.76–26.02	1.92–26.03
Observed reflections (<i>F</i> > 4 σ (<i>F</i>))	8515	16,985	8833	9786
No. of refined parameters	955	505	505	553
<i>R₁</i> ^a for significant reflections	0.0388	0.0320	0.0366	0.0469
<i>wR₂</i> ^b for significant reflections	0.0984	0.0763	0.0894	0.0813
GoF ^c	0.981	0.981	1.010	1.021

$$^a R_1 = \frac{\sum(|F_o| - |F_c|)}{\sum F_o}$$

$$^b wR_2 = \left[\frac{\sum [w(F_o^2 - F_c^2)]^2}{\sum w(F_o^2)^2} \right]^{1/2}; w = 0.0453, 0.0614, 0.0535, \text{ and } 0.0250 \text{ for } \mathbf{4aO}, \mathbf{4b}, \mathbf{4cO}, \text{ and } \mathbf{7a}, \text{ respectively.}$$

$$^c \text{GoF} = \left[\frac{\sum w(F_o^2 - F_c^2)^2}{(N_{\text{reflections}} - N_{\text{params}})} \right]^{1/2}$$

phosphine [(μ -P,P-PPh₂CH₂PPh₂)Co₂(CO)₄(μ , η -Me₂NCH₂C \equiv CPR₂)] (**4a**: R=^tBu) (or **4b**: R=Ph; **4c**: R=Cy) and a much smaller amount of [(μ -P,P-PPh₂CH₂PPh₂)Co₂(CO)₄(μ , η -Me₂NCH₂C \equiv CP(=O)R₂)] **4aO** (R=^tBu) (Scheme 1). In the absence of oxygen all three compounds, **4a**, **4b**, and **4c**, are stable in organic solvents for appreciable periods of time. Nevertheless, a small portion of **4a** slowly converted to its oxidized form **4aO** during crystallization; on the contrary, **4b** or **4c** remained almost intact. In addition, purification of **4a** by a chromatographic method on a silica support produced **4aO** in variable quantities depending on the duration of the process. Obviously, **4a**, bearing two electron-donating ^tBu groups on its phosphorus atom, is more prone to oxidation than either **4b** or **4c**. It is also evidenced by a lower isolated yield of **4a** compared to those of **4b** and **4c**. All four compounds, **4a**, **4aO**, **4b**, and **4c**, were characterized by spectroscopic methods. In addition, crystal structures of **4aO**, **4b**, and **4c** were determined by single-crystal X-ray diffraction techniques (Table 1). In the ¹H NMR spectrum of **4a**, two sets of multiplets appearing at 4.74 and 3.87 ppm correspond to the methylene protons of the coordinated dppm ligand. A singlet observed at 3.56 ppm is assigned to the methylene adjacent to nitrogen. The ³¹P NMR spectrum displays two singlets at 38.23 and 44.05 ppm. The former signal is assigned to the two equivalent phosphorus atoms of the coordinated dppm ligand; while the latter peak is assigned to the free phosphorus site. Similar assignments are also implemented for **4b** and **4c**. In **4b**, two sets of multiplets appearing at 4.33 and 3.63 ppm are attributed to the methylene protons of the coordinated dppm ligand. The two methylene protons adjacent to nitrogen give rise to a singlet at 3.51 ppm. The ³¹P NMR spectrum displays two sets of singlets at 38.01 and 4.83 ppm. Once again, the former signal is assigned to the two phosphorus atoms of the coordinated dppm ligand; while the latter, a much high-field shifted signal, is ascribed to the free phosphorus site. As to the **4c**, the methylenic protons of the coordinated dppm ligand exhibit two sets of multiplets at 4.18 and 3.38 ppm in its ¹H NMR spectrum. By contrast, only a singlet peak, at 3.35 ppm, is designated for the two methylenic protons adjacent to amine because of its chemical equality. Broad multiplets in the 2.11–1.28 ppm range are assigned to the cyclohexyl groups. In the ³¹P NMR spectrum two signals at 40.90 and 15.11 ppm are attributed to the coordinated diphenylphosphino groups of dppm and the free dicyclohexylphosphino group, respectively.

The ORTEP diagrams of **4aO**, **4b**, or **4c** depicted in Figures 1–3 manifest the presence of a pseudo-tetrahedral Co₂C₂ core typical of an alkyne-bridged dicobalt complex in each molecular structure (Table 1, Figs. 1–3). Both substituents of the bridged alkyne are bent away from the dicobalt moiety and reside on the same side as predicted by Dewar–Chatt–Duncanson's model.⁶ In this regard, **4b** and **4c** can be considered as potentially chelating cobalt-containing *P,N*-ligands. This should also be true for **4a** even though its crystal structure is not available at the moment. Oxidation of the phosphorus atom in **4aO** results in the loss of its coordinating capacity

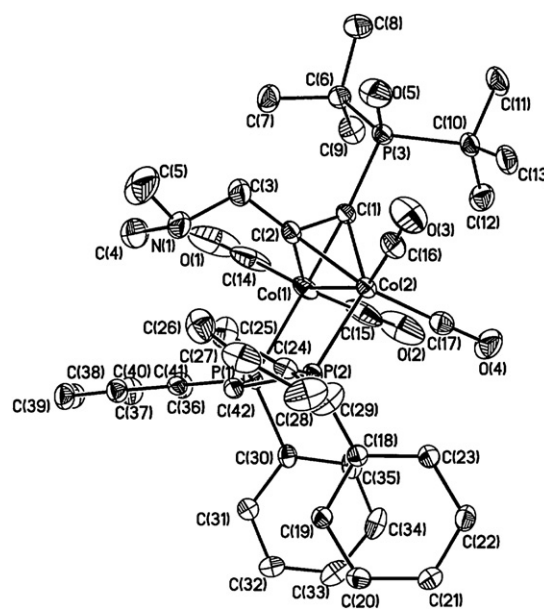


Figure 1. ORTEP drawing of **4aO**. Hydrogen atoms are omitted for clarity. Selected bond distances (Å) and angles (°): Co(1)–C(2) 1.974(3); Co(1)–C(1) 1.978(3); Co(2)–C(2) 1.956(3); Co(2)–C(1) 1.984(3); P(3)–O(5) 1.449(3); P(3)–C(1) 1.812(3); N(1)–C(3) 1.415(4); N(1)–C(4) 1.440(6); N(1)–C(5) 1.470(6); C(1)–C(2) 1.360(4); C(2)–C(3) 1.514(5); O(5)–P(3)–C(1) 110.09(15); O(5)–P(3)–C(10) 109.83(17); C(1)–P(3)–C(10) 108.84(14); O(5)–P(3)–C(6) 110.27(17); C(1)–P(3)–C(6) 107.74(14); C(10)–P(3)–C(6) 110.04(15); C(3)–N(1)–C(4) 110.6(4); C(3)–N(1)–C(5) 111.4(4); C(4)–N(1)–C(5) 108.4(4); C(2)–C(1)–P(3) 130.0(2); C(1)–C(2)–C(3) 131.4(3); N(1)–C(3)–C(2) 118.9(3).

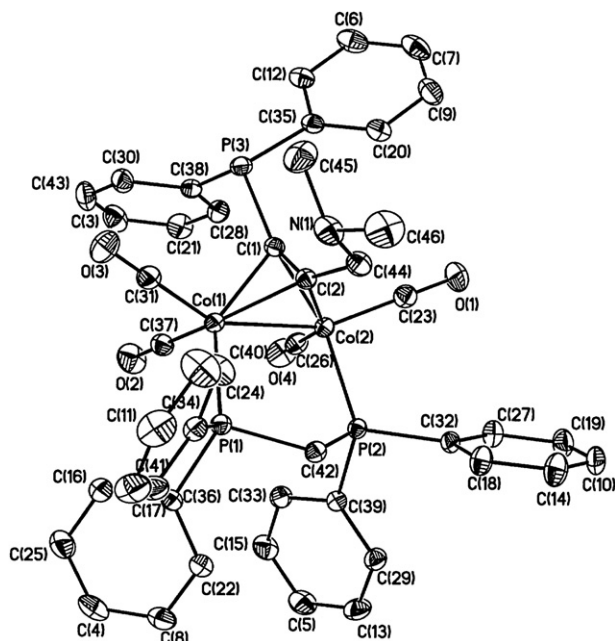


Figure 2. ORTEP drawing of **4b**. Hydrogen atoms are omitted for clarity. Selected bond distances (Å) and angles (°): Co(1)–C(1) 1.965(2); Co(1)–C(2) 1.971(2); P(3)–C(1) 1.797(2); P(3)–C(38) 1.829(2); P(3)–C(35) 1.831(2); N(1)–C(44) 1.436(3); N(1)–C(45) 1.455(4); N(1)–C(46) 1.459(4); C(1)–C(2) 1.346(3); C(2)–C(44) 1.507(3); C(1)–P(3)–C(38) 103.50(10); C(1)–P(3)–C(35) 105.26(10); C(38)–P(3)–C(35) 102.05(10); C(44)–N(1)–C(45) 112.6(2); C(44)–N(1)–C(46) 111.3(2); C(45)–N(1)–C(46) 110.7(2); C(2)–C(1)–P(3) 141.62(17); C(1)–C(2)–C(44) 140.2(2); N(1)–C(44)–C(2) 115.37(19).

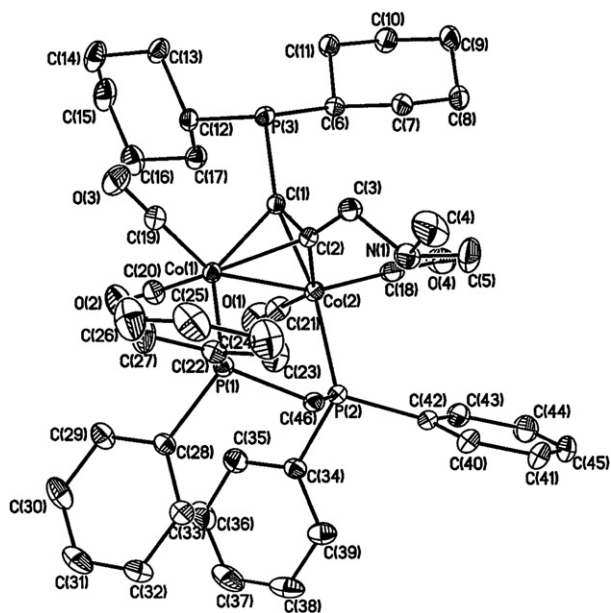


Figure 3. ORTEP drawing of **4c**. Hydrogen atoms are omitted for clarity. Selected bond distances (Å) and angles (°): P(3)–C(1) 1.806(3); P(3)–C(12) 1.855(3); P(3)–C(6) 1.862(3); N(1)–C(5) 1.458(4); N(1)–C(3) 1.460(3); N(1)–C(4) 1.469(4); C(1)–C(2) 1.351(3); C(2)–C(3) 1.512(3); C(1)–P(3)–C(12) 103.19(12); C(1)–P(3)–C(6) 101.20(11); C(12)–P(3)–C(6) 106.00(12); C(5)–N(1)–C(3) 110.8(3); C(5)–N(1)–C(4) 109.2(3); C(3)–N(1)–C(4) 108.6(3); C(2)–C(1)–P(3) 134.3(2); C(1)–C(2)–C(3) 131.4(2); N(1)–C(3)–C(2) 117.6(2).

toward a soft metal.⁷ In all structures, the dpmm and amino fragments are located on the same side of the Co₂C₂ core preventing a severe steric interaction with bulky phosphine substituents.

2.2. Complexation of **4a** with palladium

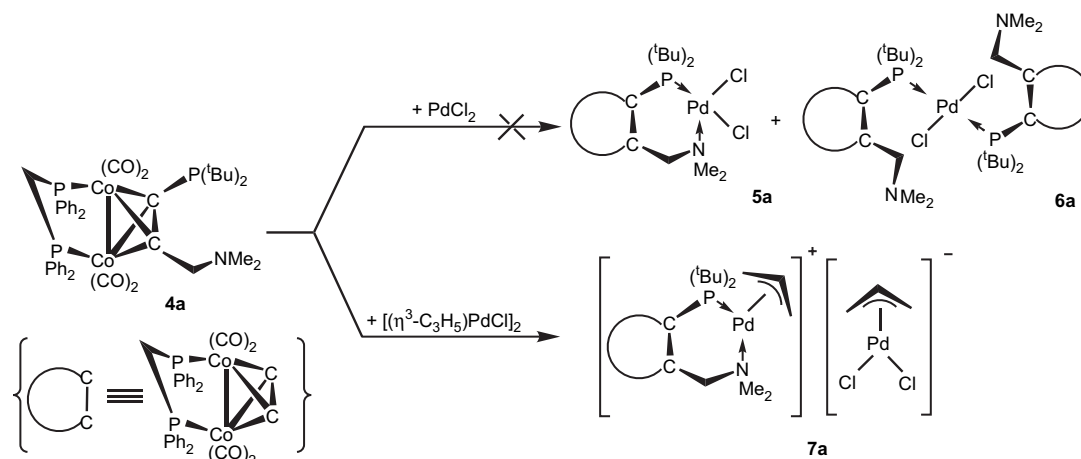
In an attempt to prepare **4a**-chelated palladium dichloride complex $(\mu\text{-PPh}_2\text{CH}_2\text{PPh}_2)\text{Co}_2(\text{CO})_4(\mu,\eta\text{-Ph}_2\text{PC}\equiv\text{CCH}_2\text{NMe}_2)\text{PdCl}_2$ **5a** or *trans*- $[(\mu\text{-PPh}_2\text{CH}_2\text{PPh}_2)\text{Co}_2(\text{CO})_4(\mu,\eta\text{-Ph}_2\text{PC}\equiv\text{CCH}_2\text{NMe}_2)]_2\text{-PdCl}_2$ **6a**, the newly made *P,N*-ligand **4a** was reacted with PdCl₂, a commonly used palladium source, in toluene at 25 °C for 0.5 h (Scheme 2). Unfortunately, numerous attempts to isolate and characterize presumed products **5a** or **6a**, including those of growing crystals suitable for X-ray analysis, were unsuccessful. In contrast to the previous result, the reaction of **4a** with a different palladium source, $([\eta^3\text{-C}_3\text{H}_5]\text{PdCl})_2$, yielded an unusual **4a**-chelated palladium complex ion pair $[(\mu\text{-PPh}_2\text{CH}_2\text{PPh}_2)\text{Co}_2(\text{CO})_4(\mu,\eta\text{-Ph}_2\text{PC}\equiv\text{CCH}_2\text{NMe}_2)\text{Pd}(\eta^3\text{-C}_3\text{H}_5)]([\eta^3\text{-C}_3\text{H}_5]\text{PdCl}_2)^-$ **7a**. Compound **7a** was characterized by spectroscopic methods (¹H, ¹³C, ³¹P NMR, and MS) and single-crystal X-ray diffraction studies. Interestingly, a similar result was obtained by Hegedus⁸ from the reaction of TMEDA with $([\eta^3\text{-C}_3\text{H}_5]\text{PdCl})_2$.

The ORTEP diagrams of both cationic and anionic parts of **7a** are depicted in Figure 4. The cationic component is comprised of a $(\eta^3\text{-C}_3\text{H}_5)\text{Pd}^+$ fragment ligated by a neutral **4a**; whereas the anionic component is the same allyl palladium moiety coordinated by two negatively charged chloride ligands. Both cation and anion of this ion pair are 16 electron complexes, which is in accord with the commonly observed palladium complexes. For the cation the bite angle of **4a** ($\angle\text{N-Pd-P}$) of 100.03(11)° is larger than most of the bite angle values reported for *P,N*-chelated palladium complexes.⁹ Unlike the Hegedus' TMEDA-chelated five-membered ring palladium complex, the **4a**-chelated cation of **7a** is a six-membered ring palladium moiety (P(1), Pd(1), N, C(3), C(1), and C(2)). As far as the anion is concerned, the Cl(2)–Pd(2)–Cl(1) angle of 97.61(6)° is well within the range of values observed for doubly-bridged chloride palladium dimers.^{9b,10} Obviously, in the case of the synthesis of **7a**, 1 molequiv of **4a** is sufficient to react with 1 molequiv of $([\eta^3\text{-C}_3\text{H}_5]\text{PdCl})_2$ dimer. Here, **4a** has proven itself as an authentic chelating *P,N*-ligand. Although some *P,N*-chelated palladium complexes are known, to the best of our knowledge, this is the first crystal structure reported for a *P,N*-chelated palladium complex cation with $([\eta^3\text{-C}_3\text{H}_5]\text{PdCl}_2)^-$ as a counter ion.¹⁰

2.3. Applications of **4a** and **4b** in palladium-catalyzed amination reactions

Suzuki reactions of arylbromides with phenylboronic acid employing various **4a**/[Pd] combinations ([Pd]: Pd(OAc)₂, PdCl₂, $([\eta^3\text{-C}_3\text{H}_5]\text{PdCl})_2$) as catalyst precursors were carried out as described elsewhere.^{11,11} Unexpectedly, the catalytic efficiencies were much lower than those observed by us previously in related studies.¹² However, application of **4a** to a palladium-catalyzed amination reaction turned out to be encouraging (Scheme 3). The results obtained are contrary to the general experimental observation that an amination reaction proceeds under much harsher condition than those of the Suzuki reaction.¹³

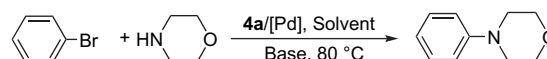
Since the performance of a successful metal-catalyzed cross-coupling reaction is known to be governed by a number of factors,¹⁴ at first the effects of various bases, temperature, and reaction time on the amination process employing **4a**/Pd(OAc)₂ were surveyed. The general procedures are shown below. A suitable Schlenk tube was charged with a magnetic stirrer then was placed with 1.0 mmol of bromobenzene, 1.2 equiv of morpholine, 1.4 equiv of a base, 1.0 mL solvent, and 1.0 mmol % of **4c**/palladium salt. The mixture was heated for certain time and workup followed. As shown in Table 2, a rather good yield (90%) was obtained when the reaction was carried out at 60 °C for 19 h or more using KF as a base (entry 1). It has also been shown that with NaO^tBu as a base the reaction reached a satisfactory yield after 24 h (entry 5). Obviously, an



Scheme 2.

induction period is needed before the reaction can reach a reasonable rate (entries 2–5). By raising temperature from 60 to 80 °C, a quantitative conversion can be achieved in a substantially shorter time period (entry 9). At the elevated temperature the best base/solvent combination is NaO^tBu/toluene (entries 7–9). As illustrated, at this temperature the reaction reaches an excellent yield in a relatively short time (entry 9). It might partly be due to the reducing capability of NaO^tBu in toluene solvent.

Next, the same amination reaction with **4a** as a ligand, NaO^tBu/toluene, and various palladium sources was carried out (Table 3). As shown, an excellent yield was obtained with either Pd₂(dba)₃, Pd(OAc)₂, or [(η³-C₃H₅)PdCl]₂ as palladium sources (entries 1, 4,



Scheme 3.

and 5). Although the latter complex is very efficient, the use of this complex is not practical due to its sensitivity to air.

Subsequently, the impact of various solvents on the reaction was evaluated. The coupling reactions were carried out under the same condition as shown in Table 3 except using Pd(OAc)₂ as the palladium source. As demonstrated, the reaction rate is greatly affected by the solvent used. The conversion rate measured by NMR are listed (THF=87.9; toluene >99; 1,4-dioxane ~0). For instance, the coupling reaction in 1,4-dioxane was ineffective. However, the yield was greatly improved when toluene was used as a solvent.

Table 2
Amination reaction using **4a**/Pd(OAc)₂ and various bases^a

Entry	Base	Temperature (°C)	Time (h)	Yield ^b (%)
1	KF	60	19	90
2	NaO ^t Bu	60	2	19
3	NaO ^t Bu	60	4	27
4	NaO ^t Bu	60	18	26
5	NaO ^t Bu	60	24	79
6	NaO ^t Bu	60	30	84
7	NaO ^t Bu	80	2	78
8	NaO ^t Bu	80	4	87
9	NaO ^t Bu	80	6	98
10	K ₂ CO ₄	80	6	52
11	KF	80	6	Trace
12	K ₂ CO ₃	80	6	Trace
13	KO ^t Bu	80	6	Trace

^a Reaction conditions: 1.0 mmol of bromobenzene, 1.2 mmol morpholine, and 1.4 mmol of base, 2.0 mL toluene, 1.0 mmol % **4a**/Pd(OAc)₂.

^b Isolated yield; determined by GC; average of two runs.

Table 3
Amination reaction using various Pd sources^a

Entry	Pd source	NMR conv. ^b (%)
1	Pd ₂ (dba) ₃	97.8
2	Pd(COD)Cl ₂	17.1
3	PdCl ₂ (CH ₃ CN) ₂	95.5
4	Pd(OAc) ₂	89.3
5	[(η ³ -C ₃ H ₅)PdCl] ₂	96.5
6	Pd(acac) ₂	90.5

^a Reaction conditions: 1.0 mmol of bromobenzene, 1.2 mmol morpholine, and 1.4 mmol of NaO^tBu, 2.0 mL toluene, 1.0 mmol % of **4a**/[Pd]=1:1, 2 h, 80 °C.

^b Average of two runs.

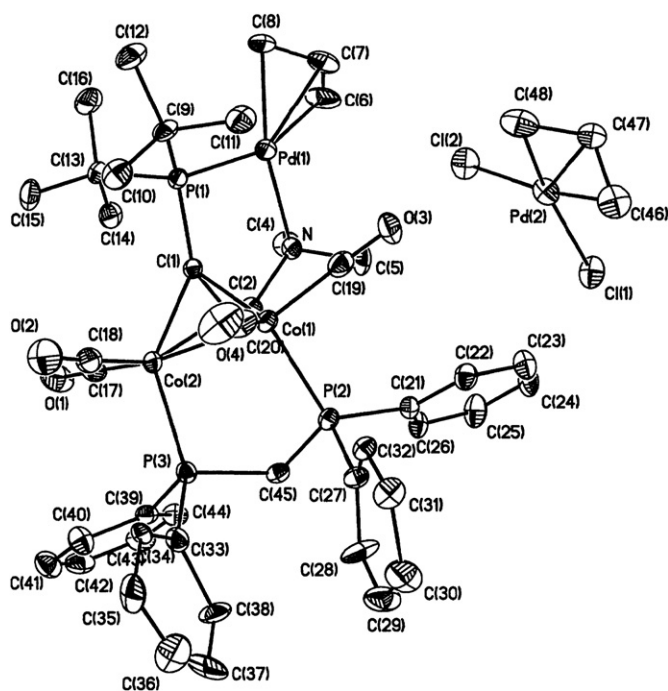


Figure 4. ORTEP drawing of **7a**. Hydrogen atoms are omitted for clarity. Selected bond distances (Å) and angles (°): Pd(1)–P(1) 2.3227(14); Pd(1)–N 2.226(4); Pd(1)–C(8) 2.105(5); Pd(1)–C(7) 2.156(7); Pd(1)–C(6) 2.233(6); P(1)–C(1) 1.801(5); N–C(3) 1.510(6); C(1)–C(2) 1.365(6); C(2)–C(3) 1.508(6); Pd(2)–C(48) 2.101(6); Pd(2)–C(47) 2.109(10); Pd(2)–C(46) 2.106(6); Pd(2)–Cl(1) 2.3856(16); Pd(2)–Cl(2) 2.3693(18); C(8)–Pd(1)–C(6) 66.5(3); C(7)–Pd(1)–C(6) 35.3(2); C(7)–Pd(1)–C(8) 38.0(2); N–Pd(1)–P(1) 100.03(11); C(48)–Pd(2)–C(47) 39.0(3); C(47)–Pd(2)–C(46) 37.1(3); C(48)–Pd(2)–C(46) 68.5(3); Cl(2)–Pd(2)–Cl(1) 97.61(6).

To establish the best ligand-to-metal ratio, the amination reaction was carried out under various **4a**/[(η^3 -C₃H₅)PdCl]₂ molar ratios and conditions shown in Table 4. The best yield was achieved with **4a**/[Pd]=1:2 (Table 4, entry 5). This observation is worth noting since it is generally believed that 2 molequiv of a monodentate phosphine ligand are required for an effective catalytic Suzuki reaction.¹⁵ Moreover, it is consistent with the molecular structure of **7a**. The catalytic efficiencies were quite different although the ratios of **4a** to palladium are the same (entries 2 and 5). It indicates that the Pd loading is also critical for efficient catalysis.

The isolated and purified **7a** was employed as the palladium source in the amination reactions of bromobenzene with morpholine. Reactions were carried out in the NaO^tBu/toluene system at 80 °C for 1 h (Table 5). As shown, the catalytic efficiency of the reaction with pre-formed complex **7a** is clearly as good as that with **7a** formed in situ. It indicates that complex **7a** is a genuine catalytically active species. In addition, the catalytic efficiency could be greatly improved upon the increase of the catalyst loading from 0.25 to 1.0 mmol% provided the reaction hours are kept the same for all cases.

Normally, for a palladium-catalyzed cross-coupling reaction a better conversion is observed with an aryl halide bearing an electron-withdrawing rather than an electron-donating substituent.¹¹ For comparison, the amination reactions of different aryl bromides, bearing electron-withdrawing/donating substituents in various positions, with morpholine and **4a**/[(η^3 -C₃H₅)PdCl]₂ as a catalyst in the NaO^tBu/toluene system were carried out (Table 6). Generally speaking, in this case the steric effect seems to be much more significant than the electronic effect, as it is clearly demonstrated by entries 3–5. Without the presence of severe steric effect, the catalytic efficiency is dominated by placing electron-withdrawing substituent on the aryl bromide. A low yield observed in entry 7 is probably due to the coordination capability of the nitrile group toward the palladium complex, which may have resulted in bypassing the major reaction route.

For comparison of catalytic efficiencies of ligands **4a** and **4b**, the amination reaction between bromobenzene and morpholine was carried out under similar conditions employing **4b**/[(η^3 -C₃H₅)PdCl]₂. The latter ligand was found to be much less efficient than **4a** (Table 7). Since a bulky ligand is favored in the reductive elimination process, this could be the rate-determining step for the whole amination reaction.

Table 4
Amination reaction under various **4a**/[(η^3 -C₃H₅)PdCl]₂ ratios^a

Entry	4a /[(η^3 -C ₃ H ₅)PdCl] ₂	Ratio of 4a /[Pd]	NMR conv. ^b (%)
1	1:0.25	1:0.5	12.7
2	0.5:0.5	0.5:1	14.6
3	1:0.5	1:1	83.1
4	2:0.5	2:1	52.6
5	1:1	1:2	97.9
6	0:0.5	0:1	trace

^a Reaction conditions: 1.0 mmol of bromobenzene, 1.2 mmol morpholine, and 1.4 mmol of NaO^tBu, 1.0 mL toluene, 1.0 mmol% of various ratios of **4a**/[(η^3 -C₃H₅)PdCl]₂, 80 °C, 1 h.

^b Average of two runs.

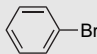
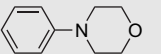
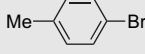
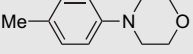
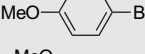
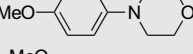
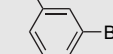
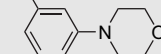
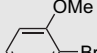
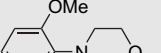
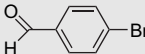
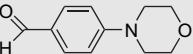
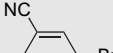
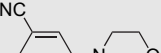
Table 5
Amination reactions employing **7a** in toluene at 80 °C^a

Entry	7a (mmol %)	NMR conv. ^b (%)
1	0.25	31.2
2	0.50	82.0
3	1.00	>99

^a Reaction condition: 1.0 mmol of bromobenzene, 1.2 mmol morpholine, and 1.4 mmol of base, 1.0 mL toluene, at 80 °C for 1 h.

^b Average of two runs.

Table 6
Dependence of the yield of the amination reaction using **4a**/[(η^3 -C₃H₅)PdCl]₂ on substrate^a

Entry	Substrate	Product	Yield ^b (%)
1			98.0
2			93.5
3			94.0
4			87.2
5			14.5
6			98.0 ^c
7			54.0

^a Reaction conditions: 1.0 mmol of aryl bromide, 1.2 mmol morpholine, and 1.4 mmol of NaO^tBu, 1.0 mmol% **4a**/[(η^3 -C₃H₅)PdCl]₂, 1.0 mL toluene, at 80 °C for 2 h.

^b Isolated yield; average of two runs.

^c Time 0.5 h.

Table 7
Dependence of the yield of the amination reaction using **4b** on the palladium source^a

Entry	Pd source	NMR conv. ^b (%)
1	Pd(OAc) ₂	6.87
2	Pd(COD)Cl ₂	10.81
3	PdCl ₂ (CH ₃ CN) ₂	11.23
4	[(η^3 -C ₃ H ₅)PdCl] ₂	34.29
5	Pd ₂ (dba) ₃	10.25
6	Pd(acac) ₂	9.20

^a Reaction condition: 1.0 mmol of bromobenzene, 1.2 mmol morpholine, and 1.4 mmol of NaO^tBu, 1.0 mL toluene, 1.0 mmol% **4b**/[Pd], 80 °C, 6 h.

^b Average of two runs.

2.4. DFT studies on the charges of the palladium centers in **7a**

As shown above, the catalytic efficiency of the reaction employing complex **7a** is as good as that carried out with **7a** formed in situ. Since the molecular structure of **7a** was shown to comprise a pair of two palladium-containing counter ions, the catalytic activity of **7a** is believed to be due to that of the **4a**-ligated palladium cationic component. The anionic part is not a major active center. Therefore, the charge distribution within **7a**, especially the charge of the palladium center of the anion, is worth checking. To the best of our knowledge, the nature of this type of the palladium complex ion pair has never been examined theoretically. Since the state-of-the-art density functional theory method (DFT) has proven itself repeatedly as a useful tool in providing reliable results in the studies of transition metal-mediated catalytic reactions, it has been employed to gain information concerning the charges of atoms in **7a**, especially those of the palladium centers. This method at the B3LYP level was utilized to examine the validity of the postulation. To make the computation feasible, a simplified model compound, **7a'**, as shown below, was selected to represent the actual reaction participant **7a** (Fig. 5). The framework of the complicated ligand **4a** was reduced to its simplest form and labeled as **4a'**. The optimized structure of **7a'** from the calculations carried out at B3LYP level of theory is shown (Fig. 6). The results of the Natural Population

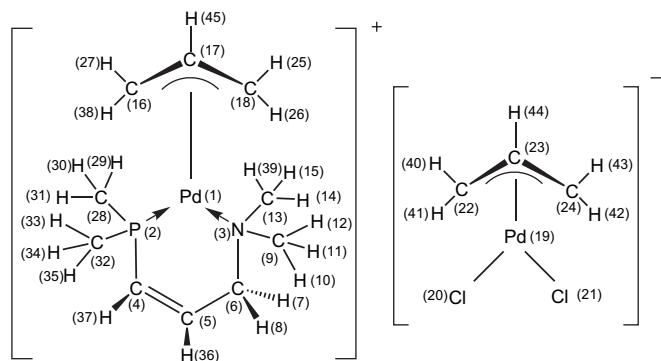


Figure 5. The Natural Population Analysis (NPA) of the atoms in **7a'**.

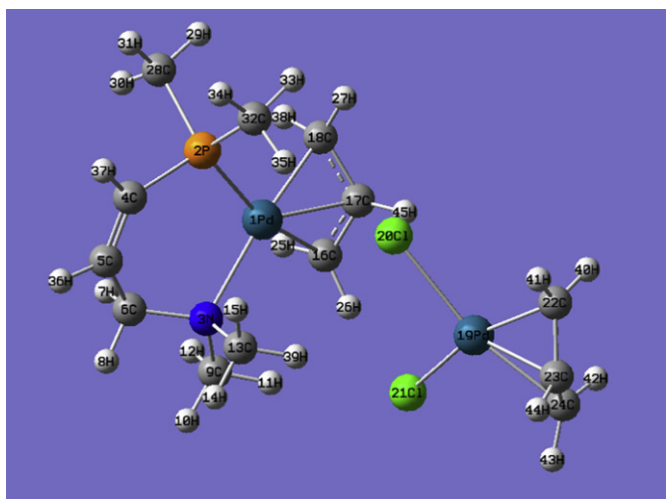


Figure 6. Optimized structure of **7a'**. The calculations were carried out at B3LYP level of theory.

Analysis (NPA) of the atomic charges in **7a'** are listed below (Table 8). As shown, the total charge of the cationic moiety is 0.90555, which is close to +1. The corresponding charge for the anionic part

Table 8
The Natural Population Analysis (NPA) of the atomic charges in **7a'** and **4a'**^a

Cationic moiety							
Metal	Pd(1)	P,N-	P(2)	N(3)	C(4)	C(5)	C(6)
	0.48602		0.90317 (0.75734)	-0.54541 (-0.52291)	-0.53143 (-0.50863)	-0.15600 (-0.18911)	-0.24883 (-0.25378)
H(7)	H(8)	C(9)	H(10)	H(11)	H(12)	C(13)	H(14)
0.23897 (0.22769)	0.20887 (0.18274)	-0.41626 (-0.41905)	0.19071 (0.17146)	0.25609 (0.21233)	0.21021 (0.21466)	-0.42310 (-0.42425)	0.18669 (0.17068)
H(15)	C(28)	H(29)	H(30)	H(31)	C(32)	H(33)	H(34)
0.21981 (0.21677)	-0.93046 (-0.94518)	0.24808 (0.23836)	0.24922 (0.23857)	0.23563 (0.21958)	-0.93301 (-0.93416)	0.25339 (0.23107)	0.22829 (0.21937)
H(35)	H(36)	H(37)	H(39)	Allyl	C(16)	C(17)	C(18)
0.28000 (0.25741)	0.22573 (0.20855)	0.23347 (0.21820)	0.26562 (0.21229)		-0.47086	-0.21723	-0.52568
H(25)	H(26)	H(27)	H(38)	H(45)			
0.21175	0.25435	0.22970	0.21978	0.26828			
Anionic moiety							
Metal	Pd(19)	Chloride	Cl(20)	Cl(21)	Allyl	C(22)	C(23)
	0.53960		-0.69037	-0.68166		-0.48281	-0.25361
C(24)	H(40)	H(41)	H(42)	H(43)	H(44)		
-0.47800	0.22208	0.22919	0.22286	0.23199	0.23518		

^a The charges of the atoms of *P,N*-ligand **4a'** are in parentheses.

is -0.90555, which is close to -1. This result is consistent with the previous assertion for the formal charge distribution within palladium complex ion pairs.⁹ The charges of Pd(19) and Pd(1) are 0.53960 and 0.48602, respectively. The less positive charge of Pd(1) is believed to be due to a donation of electron density from the phosphine site of the *P,N*-ligand. Thereby, the latter is more likely to participate in the oxidative addition process than the former, as it was expected. The charge of P(2) is 0.75734 before and 0.90317 after the coordination. Obviously, the phosphorus site donates electron density to the metal center. On the contrary, the nitrogen site pulls the electron density from the metal center. The charge of N(3) is -0.52291 before and -0.54541 after coordination. The total charges for the allyl groups of the anion and cation are -0.07312 and -0.02991, respectively. Contrary to the commonly assigned formal charge (-1) for the allyl group, in this case the allyl groups of both cation and anion are nearly neutral judging from NPA.¹⁶

3. Summary

We have developed a general route for the preparation of several fascinating cobalt-containing *P,N*-bidentate ligands. These ligands have proven to be fairly efficient in the palladium-catalyzed aryl halide amination reaction. A *P,N*-chelated palladium complex ion pair **7a** was characterized by spectroscopic means as well as single-crystal X-ray diffraction method. The results obtained for the simplified model compound **7a'** by means of Natural Population Analysis (NPA) allowed us to gain an insight into the charge distribution in **7a**.

4. Experimental section

4.1. General

All operations were performed in a nitrogen flushed glove box or in a vacuum system. Freshly distilled solvents were used. All processes of separation of the products were performed by Centrifugal Thin Layer Chromatography (CTLC, Chromatotron, Harrison model 8924) or column chromatography. GC analyses were performed on a HP-5890 FID GC with a QUADREX 007-CW fused silica 30 m column, and data were recorded on a HP ChemStation. Most

of the ^1H NMR spectra were recorded on a 300 MHz Varian VXR-300S spectrometer. In addition, some routine ^1H NMR spectra were recorded either on a Gemini-200 spectrometer at 200.00 MHz or Varian-400 spectrometer at 400.00 MHz. The chemical shifts are reported in parts per million relative to internal standards CHCl_3 ($\delta=7.26$), CH_2Cl_2 ($\delta=5.30$), or $\text{CH}_3\text{C}(=\text{O})\text{CH}_3$ ($\delta=2.09$). ^{31}P and ^{13}C NMR spectra were recorded at 121.44 and 75.46 MHz, respectively. The chemical shifts for the former and the latter are reported in parts per million relative to internal standards H_3PO_4 ($\delta=0.0$) and CHCl_3 ($\delta=77$) or CH_2Cl_2 ($\delta=53$), respectively. Mass spectra were recorded on JOEL JMS-SX/SX 102A GC/MS/MS spectrometer. Elemental analyses were recorded on Heraeus CHN-O-S-Rapid.

4.2. Synthesis and characterization of 4a–4c

Dicobalt octacarbonyl $\text{Co}_2(\text{CO})_8$ (1.00 mmol, 0.341 g), dpmm (1.00 mmol, 0.384 g), and THF (10 mL) were placed in a 100 mL round-bottomed flask charged with a magnetic stirring bar. The solution was stirred at 60 °C for 3.5 h yielding yellow-colored $\text{Co}_2(\text{CO})_6(\mu\text{-P,P-dppm})$, **3**. Without further separation, the reaction flask was charged with 1 molequiv of $\text{Me}_2\text{NCH}_2\text{C}\equiv\text{CPR}_2$ (**2a**: $\text{R}=\text{tBu}$; **2b**: $\text{R}=\text{Ph}$; **2c**: $\text{R}=\text{Cy}$) in toluene (10 mL). Subsequently, the solution was stirred at 75 °C for 48 h before the solvent was removed under reduced pressure. The residue was separated by TLC. A dark-green colored band was eluted using a mixed solvent mobile phase ($\text{CH}_2\text{Cl}_2/\text{EA}=3:1$) and was identified as **4a** (or **4b**, **4c**). The yields of **4a**, **4b**, and **4c** were 39% (0.656 g, 0.78 mmol), 55% (0.969 g, 1.10 mmol), and 63% (1.126 g, 1.26 mmol), respectively.

4.2.1. Selected spectroscopic data for 4a

^1H NMR(acetone- d_6/δ): 7.75–7.09 (m, 20, arene), 4.74 (q, $J_{\text{P-H}}=12$ Hz, 1H, dpmm), 3.87 (q, $J_{\text{P-H}}=12$ Hz, 1H, dpmm), 3.56 (s, 2H, CH_2), 2.11–2.07 (m, 6H, CH_3), 1.35 (d, 18H, $J_{\text{P-H}}=11$ Hz, ^tBu); ^{13}C NMR(acetone- d_6/δ): 128.7–132.7 (m, 24C, arene), 37.3 (t, $J_{\text{P-C}}=42$ Hz, CH_2 , dpmm), 34.9 (d, $J_{\text{P-C}}=30$ Hz, 2C, ^tBu), 28.5 (s, 6C, ^tBu); ^{31}P NMR(CDCl_3/δ): 38.23(s, 2P, dpmm), 44.05 (s, 1P, $\text{P}(^t\text{Bu})_2$).

4.2.2. Selected spectroscopic data for 4b

^1H NMR(acetone- d_6/δ): 7.69–7.15 (m, 30H, arene), 4.33 (q, $J_{\text{P-H}}=13$ Hz, 1H, dpmm), 3.63 (q, $J_{\text{P-H}}=12$ Hz, 1H, dpmm), 3.51 (s, 2H, CH_2), 2.11–2.07 (m, 6H, CH_3); ^{13}C NMR(acetone- d_6/δ): 128.9–133.3 (m, 36C, arene); ^{31}P NMR(CDCl_3/δ): 38.01 (s, 2P, dpmm), 4.83 (s, 1P, $\text{P}(\text{Ph})_2$); MS (FAB): $m/z=785$ [$\text{M}]^+$. Anal. Calcd for $\text{C}_{46}\text{H}_{45}\text{Co}_2\text{NO}_4\text{P}_3$: C, 58.30%; H, 4.94%; N, 1.13%. Found: C, 62.00%; H, 4.57%; N, 1.59%.

4.2.3. Selected spectroscopic data for 4c

^1H NMR($\text{CD}_2\text{Cl}_2/\delta$): 7.57–7.11 (m, 20H, arene), 4.18 (q, $J_{\text{P-H}}=12$ Hz, 1H, dpmm), 3.38 (q, $J_{\text{P-H}}=13$ Hz, 1H, dpmm), 3.35 (s, 2H, CH_2), 2.11–2.07 (m, 6H, CH_3), 2.11–1.28 (m, 22H, cyclohexyl); ^{13}C NMR($\text{CD}_2\text{Cl}_2/\delta$): 204.6–208.3 (s, 4C, CO), 138.3–128.4 (m, 24C, arene), 105.4 (s, 1C, $\text{P-C}\equiv\text{C}$), 96.9 (d, $J_{\text{P-H}}=65$ Hz, 1C, $\text{P-C}\equiv\text{C}$), 63.6 (s, 1C, C–N), 47.1 (s, 6C, N–C), 38.7 (t, $J_{\text{P-C}}=40$ Hz, 1C, dpmm), 27.9–25.6 (m, 12C, cyclohexyl); ^{31}P NMR(CDCl_3/δ): 40.90 (s, 2P, dpmm), 15.11 (s, 1P, $\text{P}(\text{Cy})_2$); MS (FAB): $m/z=894$ [$\text{M}]^+$. Anal. Calcd for $\text{C}_{46}\text{H}_{52}\text{Co}_2\text{NO}_4\text{P}_3$: C, 61.82%; H, 5.86%; N, 1.57%. Found: C, 60.56%; H, 5.48%; N, 1.44%.

4.2.4. Selected spectroscopic data for 4aO

^1H NMR($\text{CD}_2\text{Cl}_2/\delta$): 7.69–6.96 (m, 20, arene), 4.97 (q, $J_{\text{P-C}}=12$ Hz, 1H, dpmm), 3.60 (q, $J_{\text{P-C}}=13$ Hz, 1H, dpmm), 3.83 (s, 2H, CH_2), 2.02 (m, 6H, CH_3), 1.44 (d, 18H, $J_{\text{P-H}}=13$ Hz, ^tBu); ^{13}C NMR($\text{CD}_2\text{Cl}_2/\delta$): 206.6–203.6 (s, 4C, CO), 138.4–128.2 (m, 24C, arene), 110.4 (s, 1C, $\text{P-C}\equiv\text{C}$), 73.6 (d, $J_{\text{P-C}}=33$ Hz, 1C, $\text{P-C}\equiv\text{C}$), 65.2 (s, 1C, C–N), 47.5 (s, 6C, N–C), 38.4 (d, $J_{\text{P-C}}=63$ Hz, 2C, ^tBu) 36.3 (t, 1C, dpmm), 28.5 (s, 6C, ^tBu); ^{31}P NMR(CDCl_3/δ): 61.2 (s, 1P, $\text{P}(\text{O})(^t\text{Bu})_2$), 37.6 (s, 2P, dpmm);

MS (FAB): $m/z=858$ [$\text{M}]^+$. Anal. Calcd for $\text{C}_{42}\text{H}_{48}\text{Co}_2\text{NO}_5\text{P}_3$: C, 58.09%; H, 5.67%; N, 1.56%. Found: C, 58.82%; H, 5.64%; N, 1.63%.

4.3. Synthesis and characterization of 7a

Two reactants, $[(\eta^3\text{-C}_3\text{H}_5)\text{PdCl}]_2$ (0.01 mmol, 1.8 mg) and **4a** (0.01 mmol, 8.4 mg), were placed in a 100 mL round-bottomed flask charged with a magnetic stirring bar and toluene (5 mL). The solution was stirred at 25 °C for 0.5 h before the solvent was removed in vacuo. The yield was 99% (0.0091 mmol, 0.011 g).

4.3.1. Selected spectroscopic data for 7a

^1H NMR($\text{CD}_2\text{Cl}_2/\delta$): 7.75–7.00 (m, 20H, arene), 5.56, 5.42 (m, 2H, allylic $\text{HHC}=\text{C}(\text{H})\text{-CHH}$), 3.99 (d, $J_{\text{H-H}}=5.6$ Hz, 4H, allylic $\text{HHC}=\text{C}(\text{H})\text{-CHH}$), 2.94 (d, $J_{\text{H-H}}=12.4$ Hz, 4H, allylic $\text{HHC}=\text{C}(\text{H})\text{-CHH}$), 4.57, 3.78 (m, 2H, dpmm), 3.62 (s, 2H, $-\text{CH}_2\text{N}(\text{CH}_3)_2$), 2.50 (s, 6H, $-\text{CH}_2\text{N}(\text{CH}_3)_2$), 1.51 (d, $J_{\text{P-H}}=14.0$ Hz, 18H, ^tBu); ^{13}C NMR($\text{CD}_2\text{Cl}_2/\delta$): [cationic part]/206.3–203.3 (br, 4C, CO), 137.3–128.5 (m, 24C, arene), 119.0 (s, 1C, allylic $\text{C}=\text{C}-\text{C}$), 110.4 (s, 1C, $\text{P-C}\equiv\text{C}$), 70.8 (d, 1C, $\text{P-C}\equiv\text{C}$), 66.0 (s, 1C, C–N), 61.0 (m, 2C, allylic $\text{C}=\text{C}-\text{C}$), 45.0 (s, 6C, N–C), 39.8 (d, $J_{\text{C-P}}=16.1$ Hz, 2C, $\text{P}(^t\text{Bu})_2$), 37.5 (t, 1C, dpmm), 30.9 (s, 6C, $\text{P}(^t\text{Bu})_2$); [anionic part]/109.9 (s, 1C, allylic $\text{C}=\text{C}-\text{C}$), 55.5 (s, 2C, allylic $\text{C}=\text{C}-\text{C}$); ^{31}P NMR(CDCl_3/δ): 38.0 (s, 2P, dpmm), 72.8 (s, 1P, $\text{P}(^t\text{Bu})_2$); MS (FAB): $m/z=989$ [$\text{M}]^+$.

4.4. General procedure for amination reactions

An oven-dried Schlenk tube was charged with **4a** (8.41 mg, 0.01 mmol), $[(\eta^3\text{-C}_3\text{H}_5)\text{PdCl}]_2$ (1.80 mg, 0.005 mmol), and a base (1.4 mmol). The tube was evacuated and backfilled with nitrogen followed by the addition of an aryl bromide (1.00 mmol), toluene (1.0 mL), and morpholine (1.20 mmol). The tube was sealed with a Teflon screw cap, and the mixture was stirred at 80 °C for 2 h. After all starting materials had been consumed; the mixture was allowed to cool down to room temperature and then diluted with ether (40 mL). The resulting suspension was transferred into a separatory funnel and washed with water (10 mL). The organic layer was separated, dried with anhydrous MgSO_4 , and concentrated under reduced pressure. The crude residue was purified by TLC with hexane/ethyl acetate as a mobile phase. The solvent was removed under reduced pressure, and the yield of the eluted product was determined.

4.5. X-ray crystallographic studies

Suitable crystals of **4aO**, **4b**, **4c**, and **7a** were sealed in thin-walled glass capillaries under nitrogen atmosphere and mounted on a Bruker AXS SMART 1000 diffractometer. Intensity data were collected in 1350 frames with increasing ω (width of 0.3° per frame). The space group determination was based on a check of the Laue symmetry and systematic absences, and was confirmed using the structure solution. The structure was solved by direct methods using a SHELXTL package.¹⁷ All non-H atoms were located from successive Fourier maps and hydrogen atoms were refined using a riding model. Anisotropic thermal parameters were used for all non-H atoms, and fixed isotropic parameters were used for H atoms. Crystallographic data of **4aO**, **4b**, **4c**, and **7a** are summarized in Table 1.

5. Computational methods

All calculations were carried out using the Gaussian 03 package, in which the tight criterion (10^{-8} hartree) is the default for the SCF convergence.¹⁸ The molecular geometries were fully optimized with the hybrid B3LYP-DFT method under C_1 symmetry, in which the Becke three parameter exchange functional¹⁹ and the

Lee–Yang–Parr correlation functional²⁰ were used. The LANL2DZ including the double- ζ basis sets for the valence and outermost core orbitals combined with pseudopotential were used for Pd,²¹ and 6-31G(d) basis sets for the other atoms.

Acknowledgements

We are grateful to the National Science Council of the R.O.C. (Grant NSC 95-2113-M-005-015-MY3) for financial support.

Supplementary data

Crystallographic data for the structural analysis have been deposited with the Cambridge Crystallographic Data Center, CCDC nos. 650131, 650132, 665668, and 650133 for **4b**, **4aO**, **4c**, and **7a**. Copies of this information may be obtained free of charge from the Director, CCDC, 12 Union Road, Cambridge CB2 1EZ, UK (fax: +44 1223 336033; e-mail: deposit@ccdc.cam.ac.uk or <http://www.ccdc.cam.ac.uk>). Supplementary data associated with this article can be found in the online version, at doi:10.1016/j.tet.2008.07.076.

References and notes

- (a) Hassan, J.; Sévignon, M.; Gozzi, C.; Schulz, E.; Lemaire, M. *Chem. Rev.* **2002**, *102*, 1359; (b) Tang, W.; Zhang, X. *Chem. Rev.* **2003**, *103*, 3029; (c) Andersen, N. G.; Keay, B. A. *Chem. Rev.* **2001**, *101*, 997; (d) Bessel, C. A.; Aggarwal, P.; Marschilok, A. C.; Takeuchi, K. *J. Chem. Rev.* **2001**, *101*, 1031; (e) Barder, T. E.; Walker, S. D.; Martinelli, J. R.; Buchwald, S. L. *J. Am. Chem. Soc.* **2005**, *127*, 4685; (f) Walker, S. D.; Barder, T. E.; Martinelli, J. R.; Buchwald, S. L. *Angew. Chem., Int. Ed.* **2004**, *43*, 1871; (g) Hawtig, J. F. *Angew. Chem., Int. Ed.* **1998**, *37*, 2046; (h) Mann, G.; Hartwig, J. F. *J. Am. Chem. Soc.* **1996**, *118*, 13109; (i) Kataoka, N.; Shelby, Q.; Stambuli, J. P.; Hartwig, J. F. *J. Org. Chem.* **2002**, *67*, 5553; (j) Littke, A. F.; Dai, C.; Fu, G. C. *J. Am. Chem. Soc.* **2000**, *122*, 4020; (k) Planas, J. G.; Gladysz, J. A. *Inorg. Chem.* **2002**, *41*, 6947; (l) Hu, Q.-S.; Lu, Y.; Tang, Z.-Y.; Yu, H.-B. *J. Am. Chem. Soc.* **2003**, *125*, 2856; (m) Pickett, T. E.; Roca, F. X.; Richards, C. J. *J. Org. Chem.* **2003**, *68*, 2592; (n) Tang, Z.-Y.; Lu, Y.; Hu, Q.-S. *Org. Lett.* **2003**, *5*, 297; (o) Osborn, J. A.; Jardine, F. H.; Young, J. F.; Wilkinson, G. *J. Chem. Soc. A* **1966**, 1711; (p) Schrock, R. R.; Osborn, J. A. *J. Am. Chem. Soc.* **1976**, *98*, 2134; (q) Schrock, R. R.; Osborn, J. A. *J. Am. Chem. Soc.* **1976**, *98*, 2143; (r) Schrock, R. R.; Osborn, J. A. *J. Am. Chem. Soc.* **1976**, *98*, 4450; (s) *Applied Homogeneous Catalysis with Organometallic Compounds*; Cornils, B., Herrmann, W. A., Eds.; VCH: New York, NY, 1996; Vols. 1 and 2; (t) Noyori, R. *Asymmetric Catalysis in Organic Synthesis*; John Wiley and Sons: New York, NY, 1994; (u) Parshall, G. W.; Ittel, S. D. *Homogeneous Catalysis*, 2nd ed.; John Wiley and Sons: 1992; Chapter 8; (v) Vollhardt, K. P. C. *Acc. Chem. Res.* **1977**, *10*, 1; (w) Collins, A. N.; Sheldrake, G. N.; Crosby, J. *Chirality in Industry*; John Wiley and Sons: New York, NY, 1992; (x) Kagan, H. B. *Asymmetric Synthesis Using Organometallic Catalysts*. In *Comprehensive Organometallic Chemistry*; Wilkinson, G., Stone, F. G. A., Abel, E. W., Eds.; Pergamon: Oxford, 1982; Vol. 8, Chapter 53.
- (a) Tomori, H.; Fox, J. M.; Buchwald, S. L. *J. Org. Chem.* **2000**, *65*, 5334; (b) Nguyen, H. N.; Huang, X.; Buchwald, S. L. *J. Am. Chem. Soc.* **2003**, *125*, 11818; (c) Puddephatt, J. *Chem. Soc. Rev.* **1983**, *12*, 99; (d) Farr, J. P.; Olmstead, M. M.; Rutherford, N. M.; Wood, F. E.; Balch, A. L. *Organometallics* **1983**, *2*, 1758; (e) Farr, J. P.; Wood, F. E.; Balch, A. L. *Inorg. Chem.* **1983**, *22*, 1229; (f) Farr, J. P.; Olmstead, M. M.; Balch, A. L. *Inorg. Chem.* **1983**, *22*, 3387; (g) Zhang, Z.-Z.; Wang, H. K.; Wang, H. G.; Wang, R. J. *J. Organomet. Chem.* **1986**, *314*, 357; (h) Zhang, Z.-Z.; Wang, H. K.; Xi, Z.; Yao, X.-K.; Wang, R.-J. *J. Organomet. Chem.* **1989**, *376*, 123; (i) Zhang, Z.-Z.; Cheng, H. *Coord. Chem. Rev.* **1996**, *147*, 1.
- (a) Kurtev, K.; Ribola, D.; Jones, R. A.; Cole-Hamilton, D. J.; Wilkinson, G. *Dalton Trans.* **1980**, 55; (b) Linder, E.; Rauleder, H.; Wegner, P. *Z. Naturforsch.* **1984**, *B39*, 1224.
- Hong, F.-E.; Chang, Y.-C.; Chang, R.-E.; Lin, C.-C.; Wang, S.-L.; Liao, F.-L. *J. Organomet. Chem.* **1999**, *588*, 160.
- O'Connor, T. J.; Patel, H. A. *Can. J. Chem.* **1971**, *49*, 2706.
- (a) Dewar, M. J. S. *Bull. Soc. Chim. Fr.* **1951**, *18*, C71; (b) Chatt, J.; Duncanson, L. A. *J. Chem. Soc.* **1953**, 2939.
- (a) Pearson, R. G. *J. Am. Chem. Soc.* **1963**, *85*, 3533; (b) *Hard and Soft Acids and Bases*; Pearson, R. G., Ed.; Dowden, Hutchinson and Ross: Stroudsburg, PA, 1973; (c) Pearson, R. G. In *Chemical Hardness, Structure and Bonding*; Sen, K. D., Mingos, D. M. P., Eds.; Springer: Berlin, 1993; Vol. 80, Chapter 1.
- (a) Åkermark, B.; Åkermark, G.; Hegedus, L. S.; Zetterberg, K. *J. Am. Chem. Soc.* **1981**, *103*, 3037; (b) Hegedus, L. S.; Åkermark, B.; Olsen, D. J.; Anderson, O. P.; Zetterberg, K. *J. Am. Chem. Soc.* **1982**, *104*, 697; (c) De Munno, G.; Bruno, G.; Rotondo, E.; Giordano, G.; Lo Schiavo, S.; Piraino, P.; Tresoldi, G. *Inorg. Chim. Acta* **1993**, *208*, 67; (d) Böttcher, L.; Scholz, A.; Walther, D.; Weisbach, N.; Görls, H. *Z. Anorg. Allg. Chem.* **2003**, *629*, 2103.
- Crystal structures for related compounds are available from the literature: (a) Fernández-Galán, R.; Jalón, F. A.; Manzano, B. R.; Rodríguez-de la Fuente, J.; Vrahani, M.; Jedlicka, B.; Weissensteiner, W.; Jogl, G. *Organometallics* **1997**, *16*, 3758; (b) Vasconcelos, I. C. F.; Rath, N. P.; Spilling, C. D. *Tetrahedron: Asymmetry* **1998**, *9*, 937; (c) Wang, Y.; Li, X.; Sun, J.; Ding, K. *Organometallics* **2003**, *22*, 1856; (d) Faller, J. W.; Sarantopoulos, N. *Organometallics* **2004**, *23*, 2008; (e) Goldfuss, B.; Löschmann, T.; Rominger, F. *Chem.—Eur. J.* **2004**, *10*, 5422.
- Crystal structures for related compounds are available from the literature: Ref. 8c.
- (a) Yin, J.; Rainka, M. P.; Zhang, X. X.; Buchwald, S. L. *J. Am. Chem. Soc.* **2002**, *124*, 1162; (b) Netherton, M. R.; Dai, C.; Neuschütz, K.; Fu, G. C. *J. Am. Chem. Soc.* **2001**, *123*, 10099; (c) Suzuki, A. *J. Organomet. Chem.* **1999**, *576*, 147; (d) Miyura, N.; Suzuki, A. *Chem. Rev.* **1995**, *95*, 2457.
- (a) Gan, Y.-H.; Lee, J.-C.; Hong, F.-E. *Polyhedron* **2006**, *25*, 3555; (b) Lai, Y.-C.; Chen, H.-Y.; Hung, W.-C.; Lin, C.-C.; Hong, F.-E. *Tetrahedron* **2005**, *61*, 9484; (c) Chang, C.-P.; Huang, Y.-L.; Hong, F.-E. *Tetrahedron* **2005**, *61*, 3835; (d) Hong, F.-E.; Ho, Y.-J.; Chang, Y.-C.; Huang, Y.-L. *J. Organomet. Chem.* **2005**, *690*, 1249.
- (a) Wolfe, J. P.; Wagaw, S.; Buchwald, S. L. *J. Am. Chem. Soc.* **1996**, *118*, 7215; (b) Driver, M. S.; Hartwig, J. F. *J. Am. Chem. Soc.* **1996**, *118*, 7217.
- (a) Goldman, E. R.; Medintz, I. L.; Whitley, J. L.; Hayhurst, A.; Clapp, A. R.; Uyeda, H. T.; Deschamps, J. R.; Lassman, M. E.; Mattoussi, H. *J. Am. Chem. Soc.* **2005**, *127*, 6744; (b) Braga, A. A. C.; Morgon, N. H.; Ujaque, G.; Maseras, F. *J. Am. Chem. Soc.* **2005**, *127*, 9298.
- Uenishi, J.-I.; Beau, J.-M.; Armstrong, R. W.; Kishi, Y. *J. Am. Chem. Soc.* **1987**, *109*, 4756.
- Crabtree, R. H. *The Organometallic Chemistry of the Transition Metals*, 4th ed.; John Wiley and Sons: New York, NY, 2005; Chapter 5.
- Sheldrick, G. M. *SHELXTL PLUS User's Manual. Revision 4.1*; Nicolet XRD Corporation: Madison, WI, USA, 1991.
- Frisch, M. J.; Trucks, G. W.; Schlegel, H. B.; Scuseria, G. E.; Robb, M. A.; Cheeseman, J. R.; Montgomery, J. A., Jr.; Vreven, T.; Kudin, K. N.; Burant, J. C.; Millam, J. M.; Iyengar, S. S.; Tomasi, J.; Barone, V.; Mennucci, B.; Cossi, M.; Scalmani, G.; Rega, N.; Petersson, G. A.; Nakatsuji, H.; Hada, M.; Ehara, M.; Toyota, K.; Fukuda, R.; Hasegawa, J.; Ishida, M.; Nakajima, T.; Honda, Y.; Kitao, O.; Nakai, H.; Klene, M.; Li, X.; Knox, J. E.; Hratchian, H. P.; Cross, J. B.; Bakken, V.; Adamo, C.; Jaramillo, J.; Gomperts, R.; Stratmann, R. E.; Yazyev, O.; Austin, A. J.; Cammi, R.; Pomelli, C.; Ochterski, J. W.; Ayala, P. Y.; Morokuma, K.; Voth, G. A.; Salvador, P.; Dannenberg, J. J.; Zakrzewski, V. G.; Dapprich, S.; Daniels, A. D.; Strain, M. C.; Farkas, O.; Malick, D. K.; Rabuck, A. D.; Raghavachari, K.; Foresman, J. B.; Ortiz, J. V.; Cui, Q.; Baboul, A. G.; Clifford, S.; Cioslowski, J.; Stefanov, B. B.; Liu, G.; Liashenko, A.; Piskorz, P.; Komaromi, I.; Martin, R. L.; Fox, D. J.; Keith, T.; Al-Laham, M. A.; Peng, C. Y.; Nanayakkara, A.; Challacombe, M.; Gill, P. M. W.; Johnson, B.; Chen, W.; Wong, M. W.; Gonzalez, C.; Pople, J. A. *Gaussian 03, Revision B.04*; Gaussian: Wallingford, CT, 2004.
- Becke, A. D. *J. Chem. Phys.* **1993**, *98*, 5648.
- Lee, C.; Yang, W.; Parr, R. G. *Phys. Rev. B* **1988**, *37*, 785.
- (a) Dunning, T. H., Jr.; Hay, P. J. *Modern Theoretical Chemistry*; Plenum: New York, NY, 1976; (b) Hay, P. J.; Wadt, W. R. *J. Chem. Phys.* **1985**, *82*, 299.